Sustainable Energy & Fuels

Low Temperature Recovery of Acetone-Butanol-Ethanol (ABE) Fermentation Products via Microwave Induced Membrane Distillation on Carbon Nanotube Immobilized Membranes

Journal:	*Sustainable Energy & Fuels*
Manuscript ID	SE-ART-03-2020-000461.R1
Article Type:	Paper
Date Submitted by the Author:	17-Apr-2020

Complete List of Authors:	Gupta, Oindrila; New Jersey Institute of Technology, Chemistry & Environmental Science Roy, Sagar; New Jersey Institute of Technology, Chemistry & Environmental Science Mitra, Somenath; New Jersey Institute of Technology, Chemistry and Environmental Science

Low Temperature Recovery of Acetone-Butanol-Ethanol (ABE) Fermentation Products via Microwave Induced Membrane Distillation on Carbon Nanotube Immobilized Membranes

Oindrila Gupta, Sagar Roy and Somenath Mitra*

Department of Chemistry and Environmental Science,
New Jersey Institute of Technology
Newark, NJ, 07102
USA

* Corresponding Author
Somenath Mitra, 973-596-5611(t), 973-596-3586(F), somenath.mitra@njit.edu

Abstract:

Acetone, butanol and ethanol (ABE) mixture separation from dilute aqueous fermentation products is an important process for the biofuel industry. Here, we present a novel approach for ABE recovery using microwave induced membrane distillation (MD). Carbon nanotube (CNTs) and octadecyl amide (ODA) functionalized CNTs were immobilized on membrane surfaces and were used in sweep gas MD separation of ABE. The ABE flux, separation factor and mass transfer coefficient obtained with CNT and CNT-ODA immobilized membranes were remarkably higher than the commercial pristine membrane at various experimental conditions. The ABE flux enhancement reached as high as 105, 100 and 375% for CNIM and 63, 62 and 175% for CNIM-ODA respectively. ABE flux obtained was nearly ten times higher than that reported previously for pervaporation. The mass transfer coefficient also increased significantly along with a lower activation energy for the modified membranes. Mechanistically speaking, the immobilization of the carbon nanotubes on the active membrane layer led to preferential sorption of ABE leading to enhanced separation. This phenomenon has been validated by the reduction of contact angles for the aqueous ABE mixtures on the CNT and CNT-ODA immobilized membranes indicating enhanced interaction of the ABE on the membrane surface.

Keywords: ABE recovery; Sweep Gas Membrane distillation; Microwave heating; Carbon nanotubes; Mass transfer coefficient

1. Introduction

The cost-efficient production of biofuels from biomass has the potential to address global problems such as energy security and climate change. An important process in the biofuel industry is the generation of acetone-butanol-ethanol (ABE) mixture as fermentation products which has garnered huge attention in recent times [1]. There is significant interest in the efficient ethanol recovery from fermentation broths for clean fuel and chemical feed stock production [2-3]; acetone and butanol are important solvents that also have many other industrial applications[4-5]. As a biofuel, butanol has high energy content, is compatible with prevailing gasoline supply channels and has low vapor pressure [6]. In a typical ABE fermentation system, the produced acetone, butanol and ethanol maintain a fixed ratio of 3:6:1. Maximum amount of total solvents usually varies between 16-20 g/L with concentration of butanol at 10-12 g/L being a limiting factor due to end production inhibition resulting from its toxicity. This leads to high energy cost for ABE recovery from the low concentration fermentation broth via thermal distillation [7]. Currently an equivalent of 50% of the heat of combustion of butanol is used up in the ABE distillation process itself, therefore the development of cost effective separation technologies that can perform a substantial role in increasing productivity and improve the economics of ABE production is of great importance [7-9].

Alternate ABE separation approaches such as adsorption [10], gas stripping [11], liquid–liquid extraction[12], perstraction [13], pervaporation [14], membrane distillation[15] and reverse osmosis[16] have been explored. Membrane distillation (MD) is a thermally driven process where separation of two phases (a hot feed side phase and a colder receiving phase) occurs through a hydrophobic microporous membrane. The difference in temperature between the feed and permeate side of the membrane creates the vapor pressure gradient, triggering the transport of the vapor across the membrane. Some of the major advantages of MD are comparatively low energy requirement, capital cost and operation temperatures compared to distillation [17], and significantly higher flux than pervaporation . While modelling studies showed that MD has much potential in ABE separation[18-19], to the best of our knowledge, only limited experimental studies have been published in this field [15, 20].

A range of separation applications such as pervaporation, extraction, protein separation, breaking oil-water emulsion, nanofiltration and membrane distillation have been carried out on carbon nanotubes based membranes [21-28]. We have demonstrated that on immobilizing CNTs on the membrane surface, the physicochemical interaction between the solutes and the membrane can be significantly altered [24, 29-30]. A rapid progress in MD has been achieved with the incorporation of carbon nanotube immobilized membrane (CNIM) for desalination where the CNTs enhance the preferential passage of the water vapor molecules while repelling the liquid salt-water feed mixture resulting in a remarkable increase in pure water flux. Super-hydrophobic CNT loaded PVDF membrane synthesized by one-step electrospinning technique has shown improved desalination performance[31]. CNIM has been successfully implemented in membrane distillation using sweep gas to carry out the permeated species (SGMD) for enhanced organic solvent recovery [30]. Another study investigated the performance of vertically aligned (VA) and open-ended CNT arrays filled polydimethylsiloxane (PDMS) composite membrane for pervaporative recovery of butanol from ABE fermentation broth[32].

Microwave induced heating has been employed in several methods including drying, chemical synthesis and in home kitchens. Microwave processes are associated with nonthermal effects such as localized super heating, activation energy reduction, break down of hydrogen bonded structures in aqueous medium, and the generation of nano-bubbles[33-34]. Recently, a MD process induced by a microwave has been reported by our group for desalination where microwave heating led to the breakdown of hydrogen bonded salt water clusters leading to high flux[35]. Comparison of MD by conventional and microwave heating has been published before with ethanol-water system. Microwave induced membrane distillation has shown significant advantages including higher flux, selectivity and lower energy consumption[36]. Since ABE consists of polar molecules, it is anticipated that they will absorb microwave energy and their interactions will lead to the breakdown of water-organic clusters to enhance the removal of ABE[37-38]. The aim of this project was to incorporate CNIM along with microwave heating to enhance ABE separation via SGMD.

2. Experimental

2.1. Chemicals and materials

The solvents (acetone (AR ≥ 99.5%), butanol (anhydrous, 99.8%) and ethanol (anhydrous, ≥ 99.5%)) used in this experiment were procured from Sigma Aldrich (St. Louis, MO). Cheap Tubes Inc. (Brattleboro, VT) has supplied the MWCNTs (~30 nm dia, 15 μm long). Octadecyl amide ($-CO-NH-C_{18}H_{37}$) functionalization (CNT-ODA) was performed in our laboratory following a method published before [39]. In all experiments, deionized water (Barnstead 5023, Dubuque, Iowa) has been used.

2.2. CNIM and CNIM-ODA Fabrication

Proper dispersion of CNTs and CNT-ODA in organic solvent and the fabrication of uniformly distributed CNTs throughout the membrane surface was the main concern. A commercial PTFE membrane (Advantec, 0.2 μm pore size, 74% porosity, polypropylene supported) was used as base membrane and the CNIMs were prepared on it. The CNTs as well as CNT-ODA dispersion were carried out using a procedure described in our previous paper [23]. Our previous studies have indicated that functionalization of CNTs enhanced its dispersibility in the solvent phase, which eventually helped in film-formation [39]. Scanning electron microscopy (SEM) (JEOL; model JSM-7900F) was utilized to characterize the CNIM and CNIM-ODA. The hydrophobic nature of the membranes used was measured via contact angle and liquid entry pressure (LEP) measurements with DI water and ABE mixture. Drops of a fixed ABE concentration were placed on the membrane with the help of a micro syringe (Hamilton, 0–100 μL). The contact angles of the drops on the membrane surface were measured using a digital video camera placed at the top of a stage.

2.3. Experimental Set Up

Figure 1 illustrates the experimental setup. The MIMD in sweep gas mode was used in all experiments where dried air at room temperature was passed through the permeate side of the membrane module that assisted in removal of the permeated vapor. A module made of polytetrafluoroethylene (PTFE) was used in the SGMD test cell. Details have been described elsewhere [23]. The inner diameter of the module was 4.3 cm with an operational contact area of 12.5 cm^2. The ABE-water feed mixture was pumped (Cole Parmer, model 77200-52) through the SGMD module and was recirculated. The ABE-water feed temperature was controlled using a microwave oven and the power level of the microwave was adjusted as needed to get the desired temperature. The feed reservoir temperature was maintained by regulating the temperature of a constant temperature bath. A flowmeter (model no EW-03217-02, Cole Parmer) was used to monitor the sweep gas flow rate. Two thermistor thermocouples (K-type, Cole Parmer) were placed on the stream inlet and outlet to measure the temperature of the feed solution entering and exiting the membrane module.

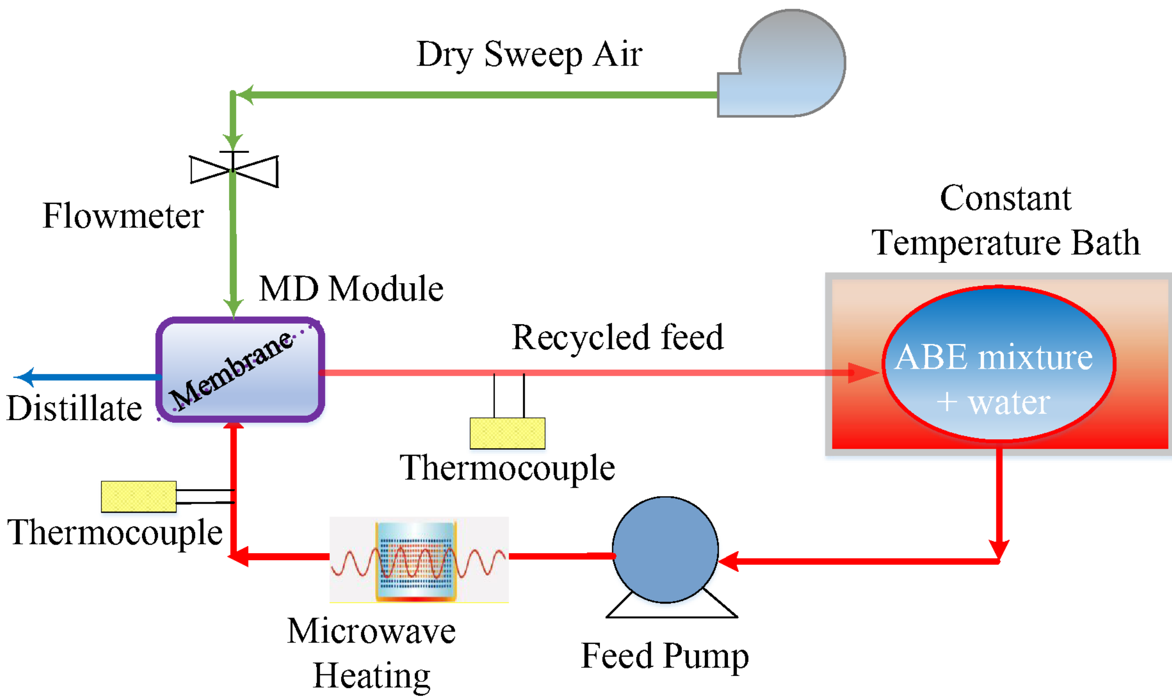

Figure 1. Experimental Setup

In order to remove impurities in the dry sweep air such as dust or moisture, laboratory air from the fume hood was circulated through a drying unit (W. A. Hammond Drierite, Xenia, OH) and hollow Fiber Filter (Barnstead International, Beverly, MA) prior to flow into the permeate side. The drying unit helps to lower the relative humidity close to zero. In all experiments, the sweep airflow rate on the permeate side was maintained 4.5L/min. Experiments were performed thrice to estimate precision. The experimental data show lower than 1% relative standard deviation.

The liquid entry pressure (LEP) is the minimum pressure at which liquid penetrates into the membrane pores. In MD, LEP measurement is important as a liquid–vapor interface develops at the membrane pore entrance and the permeated species vaporizes through it. The LEP was measured using a method described before[23]. A stainless steel chamber (Alloy Products Corp, 185 Psi Mawp) was filled with the ABE-water feed solution (1.5, 3, 0.5 vol% ABE, respectively). The membrane held in a test cell was connected to the liquid chamber. A gas cylinder was used to increase the pressure above the liquid, which was increased till the liquid started to enter through the membrane pores.

A graduated measuring cylinder was used to measure the volume of the feed solution before and after experiments. After each experiment, the recycled feed mixture was cooled down to room temperature and the final volume was measured. An airtight feed solution chamber was used to confirm that sample was not lost due to evaporation of volatile components. The flux and separation factor were calculated by analyzing the initial and final feed mixture compositions using a Gas Chromatography (HP-5890) equipped with an FID detector. The gas chromatograph was operating with injection port temperature of 200°C, column temperature of 150°C and detector temperature of 250 °C. Analyses were carried out on an EzChrom Elite Chromatography data system used for GC control, data acquisition and processing.

3. Results and discussion

The SEM images of the PTFE, CNIM, and CNIM-ODA are shown in Figure 2a, b and c. The porous structure of the pristine PTFE membrane and presence of CNT and CNT-ODA on the CNIM and CNIM-ODA surfaces are clearly visible. Uniform distribution of CNTs over the entire membrane surface was also observed. In our previous studies, gas permeation test showed no significant change in effective porosity over pore length of the membrane as very small amount of CNTs had been used to fabricate the membrane[24].

Thermogravimetric analysis (TGA) (10 ^{0}C/ min heating rate in air) was used to analyze the stability of the PTFE membrane, CNIM and CNIM-ODA at higher temperature. The TGA and differential TGA curves are shown in Figure 3a and b, respectively. It is observed that the initial thermal decomposition of the membrane began at ~260 ^{0}C (degradation of PP support layer), followed by the degradation of PTFE active layer at 500 °C. From the figure, it is evident that CNIM and CNIM-ODA were thermally stable within the operating temperature ranges.

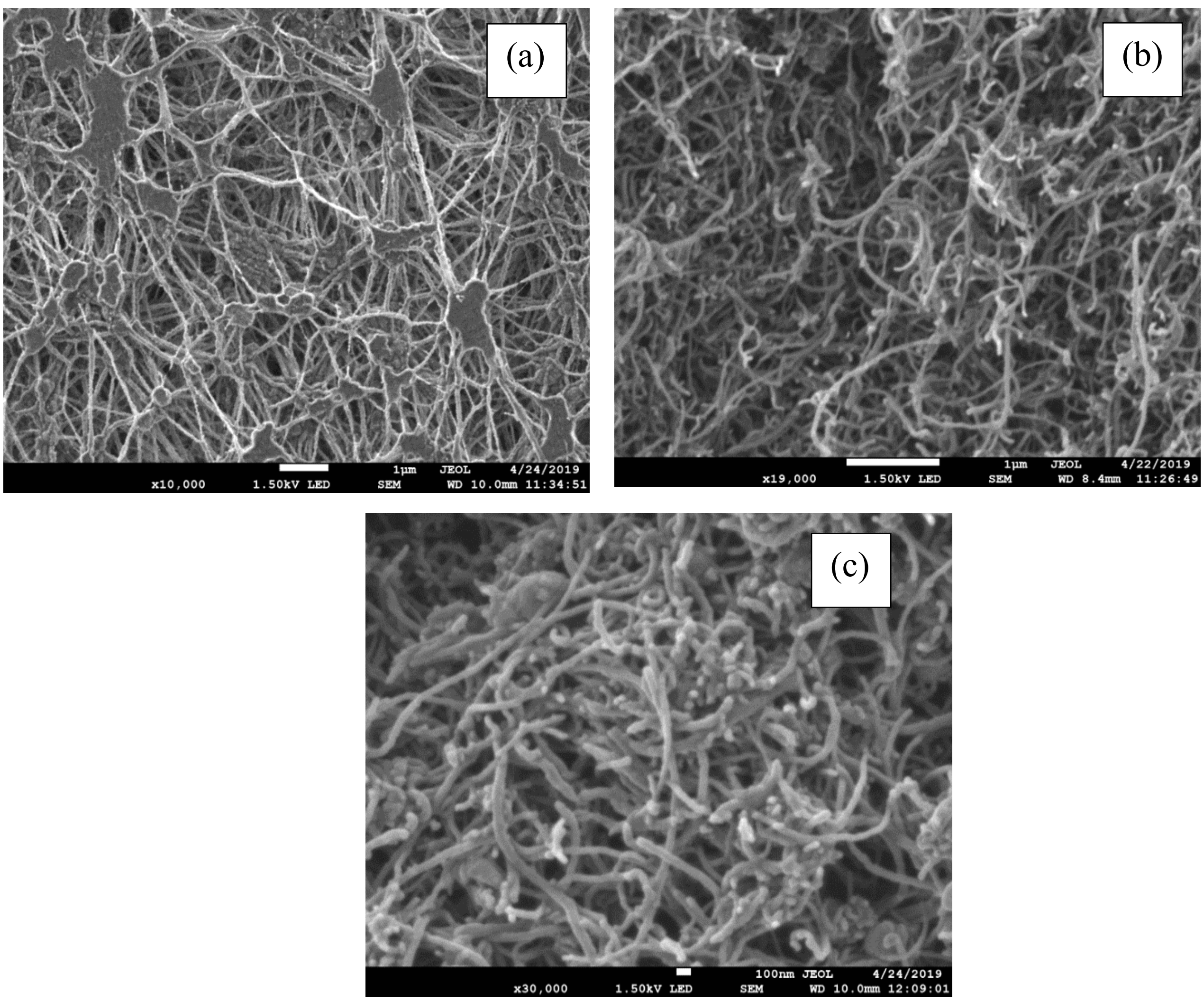

Figure 2. Scanning Electron Micrograph of (a) PTFE; (b) CNIM (c) CNIM-ODA

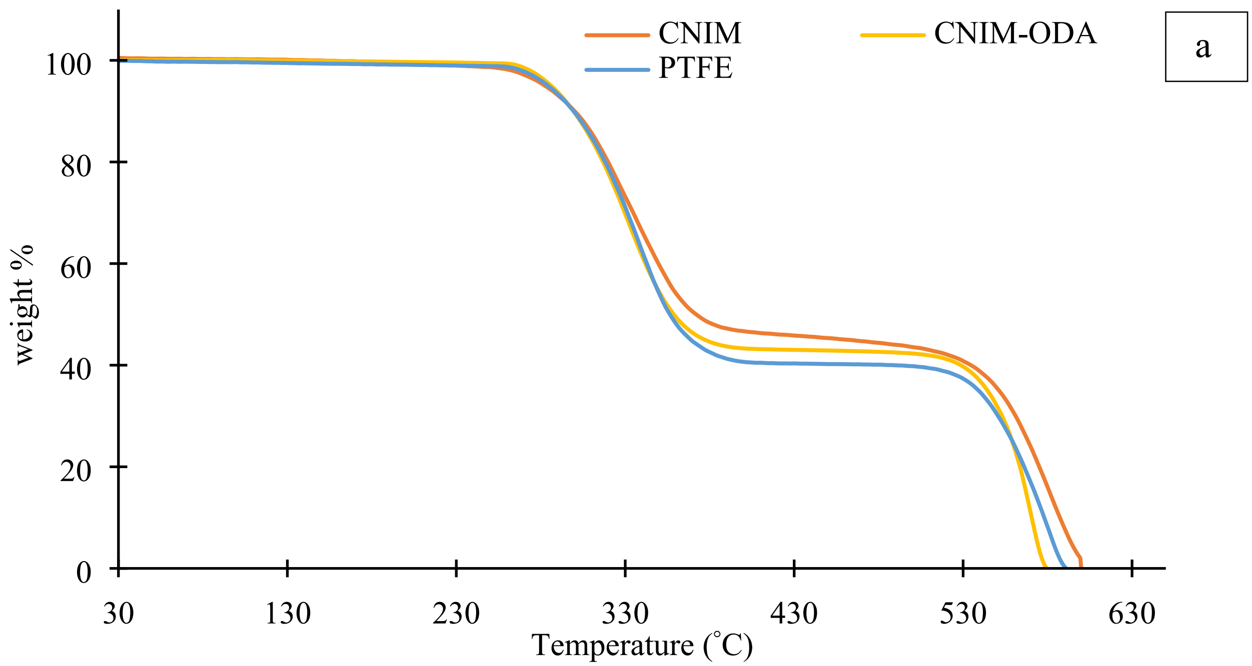

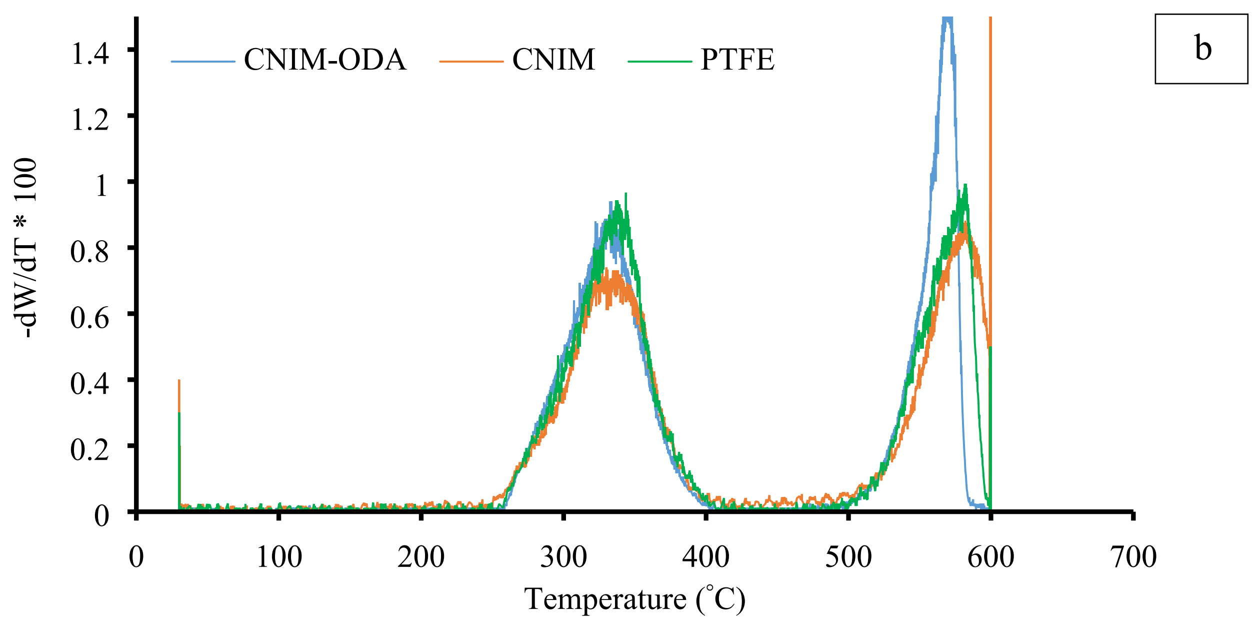

Figure 3. (a) Thermogravimetric analysis of PTFE, CNIM & CNIM-ODA; (b) differential TGA curves of the corresponding membranes.

The contact angle measurements provide a measure of wettability of the membrane surface. The contact angle depends upon the intermolecular interactions between the membrane surface and the liquid placed on it. Table 1 demonstrates the contact angle values for pure water and ABE mixtures on different membrane surfaces. As can be seen from the table, the contact angles for pure water were much higher on CNIM and CNIM-ODA due to their higher hydrophobicity which were similar to what has been reported previously [23, 29, 40]. The contact angles on the PTFE, CNIM and CNIM-ODA membranes at 0.6, 1.2 and 0.2 vol % of ABE and 97.8 % water are shown in Figure 4a, b and c. The presence of CNTs dramatically altered the contact angle for CNIM. The presence of organic molecules in aqueous solution reduced the contact angle for all membranes. However, since the alcohols and other organic solvents possess an affinity for CNTs, the contact angles of the ABE mixtures decreased significantly in CNIM and CNIM-ODA (Table 1). The contact angles for ABE mixture decreased in the following order: PTFE> CNIM-ODA> CNIM. For instance, the droplet of ABE-water mixture on CNIM indicated a contact angle of 84° vs a contact angle of 103^{0} for PTFE and 108^{0} indicating strong interactions with the CNTs and relatively less with CNT-ODA. The increasing ABE affinity to CNIM and CNIM-ODA over PTFE are potential means to increase the removal efficiency and reduce concentration polarization[41].

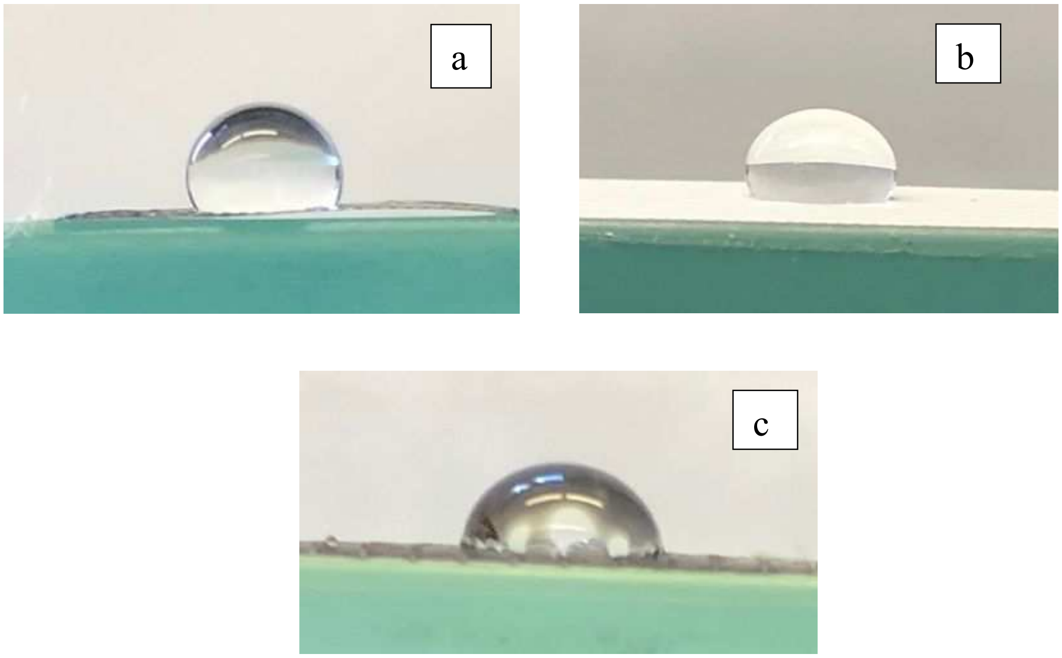

Figure 4. Picture of ABE- water solution (0.6, 1.2 and 0.2 vol % respectively) droplet on (a) CNIM-ODA; (b) PTFE; (c) CNIM

Table 1. Contact Angles of pure water & ABE mixture

Solvent	Contact angle (°)		
	PTFE	CNIM	CNIM-ODA
Pure water	105	109	116
ABE mixture	103	84	110

The LEP of pure water for PTFE, CNIM and CNIM-ODA were found to be similar, ~455.1 kPa, for all membranes, which further decreased to 220.7, 144.8 and 179.3 kPa, respectively for ABE mixture (1.5, 3 and 0.5 vol% of ABE in water). The high LEP values indicate the low wettability of the membranes as also evident from the contact angle measurement described above.

Figures 5a, b and c show the AFM images of pristine PTFE membrane, CNIM and CNIM-ODA, respectively. The average surface roughness (Ra) values was measured over an area of 10µm × 10 µm of the corresponding membrane samples and was found to be 127 nm, 142 nm and 138 nm, respectively. It is clear from the figure that the incorporation of small amount of CNTs change the surface topography significantly and alters the characteristics of the fabricated membrane surface.

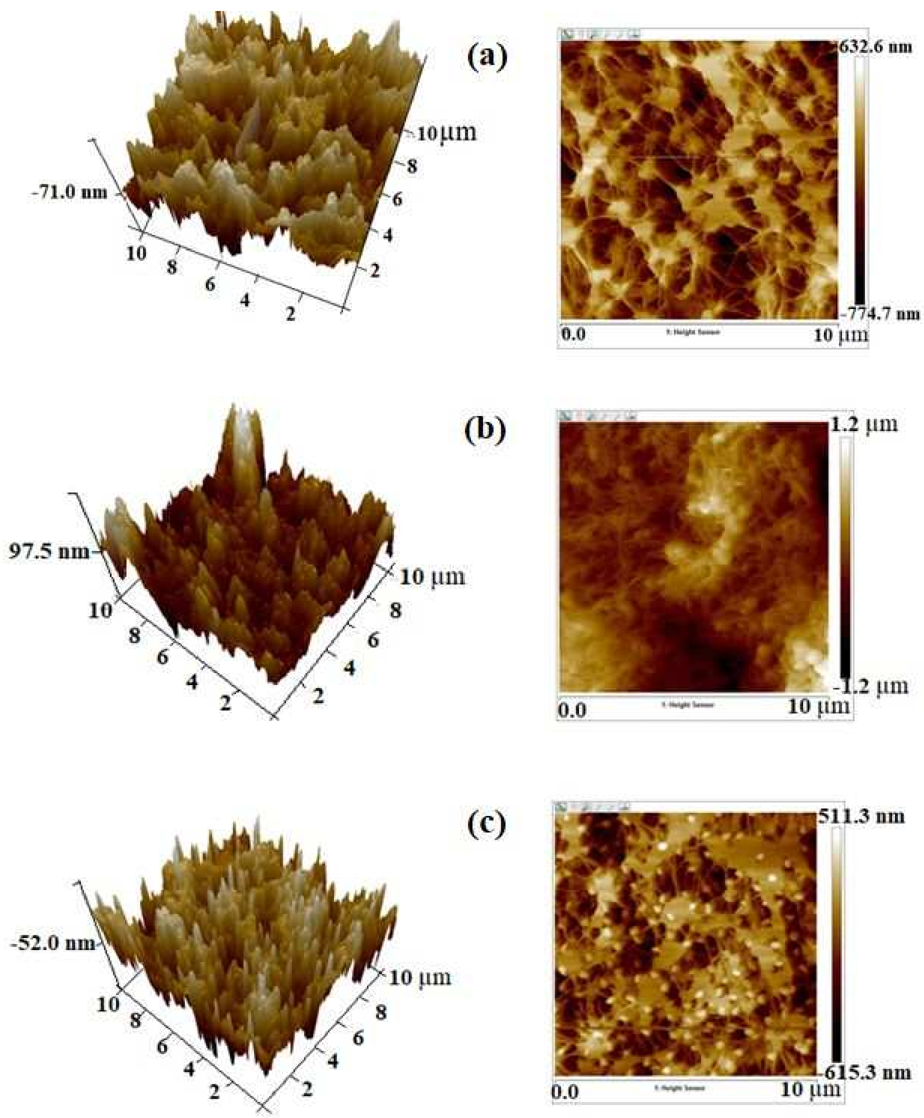

Figure 5. AFM images featuring the topography of the (a) unmodified membrane surface (PTFE); (b) CNIM and (c) CNIM-ODA

3.1. MIMD separation performance study of CNIM, CNIM-ODA and PTFE membrane

The separation performances of various membranes were characterized with respect to ABE permeation rate and selectivity. The fabricated membranes' performance were compared with the pristine membrane. The individual flux of '*i*' component (J_{wi}), was described as:

$$J_{wi} = \frac{W_{pi}}{t * A} \qquad (2)$$

Where, W_{pi} was the amount of permeated mass of species 'i' within a period of time 't' through a membrane of area 'A'. The measure of separation efficiency was denoted by separation factor (β_{i-j}), and is calculated from the following relation:

$$\beta_{i-water} = \frac{y_i / y_{water}}{x_i / x_{water}} \qquad (3)$$

where y_i and x_i represent the permeate and feed side weight fraction of 'i' component.

Apparent activation energy (Eapp) of solvent transport in the membrane processes can be expressed as [42]

$$J = J_0 \, exp\left(-\frac{E_{app}}{RT_f}\right) \qquad (4)$$

Where J and J_0 are fluxes (mol m^{-2} h^{-1}), R is gas constant (J mol^{-1} K^{-1}), T_f denotes feed temperature (K).

The Figures 6a, b and c display the effect of feed concentration on acetone, butanol and ethanol flux and separation factor. The ratio of ABE in the aqueous feed mixtures was kept constant at 3:6:1 (vol %). Three different feed concentrations namely 0.6, 1.2, and 1.5 (vol %) of acetone were tested and the butanol and ethanol in the feed solutions were adjusted accordingly. The feed temperature and feed flow rate was maintained at 40^0C and 112 mL/min, respectively. It can be observed from the figures that with increase in acetone, butanol and ethanol concentration in feed, the ABE flux increased for all membranes. The CNIM and CNIM-ODA showed improved flux compared to the PTFE membrane, which was due to the enhanced solvent affinity with the nanotubes. Total solvent flux were in the order of CNIM> CNIM-ODA> PTFE. The highest total solvent flux for CNIM may be attributed to the higher solvent sorption capacity, as also supported by the contact angle values. The presence of bulky ODA groups on CNT-ODA may have limited the direct sorption and fast transport of the organic compounds on the CNT framework.

The solvent flux reached as high as 0.82, 1.36 and 0.19 L/m^2.h for acetone, butanol and ethanol, respectively, at 40 ^{0}C and 1.5, 3 and 0.5 vol % of ABE in the feed. The CNTs influenced the acetone, butanol and ethanol partition coefficient, and its effects were more pronounced at higher concentrations. The enhancement in acetone flux reached as high as 130.3 % for CNIM and 60.6 % for CNIM-ODA over PTFE membrane at 1.2 volume % of acetone. Enhancement in butanol and ethanol flux followed similar pattern with enhancement reaching up to 127% and 375% respectively for CNIM. Figures 6 d, e, and f show plots of separation factor of ABE with respect to feed concentration. As can be seen from the plots, the separation factor was inversely proportional to the concentration for all the membranes. However, a higher separation factor for CNIM than CNIM-ODA and PTFE membrane was observed at all feed concentrations tested here. Enhancement over PTFE membrane for acetone reached as high as 79.92% for CNIM and 41.5% for CNIM-ODA. Similar trends were observed for ethanol and butanol separation factor.

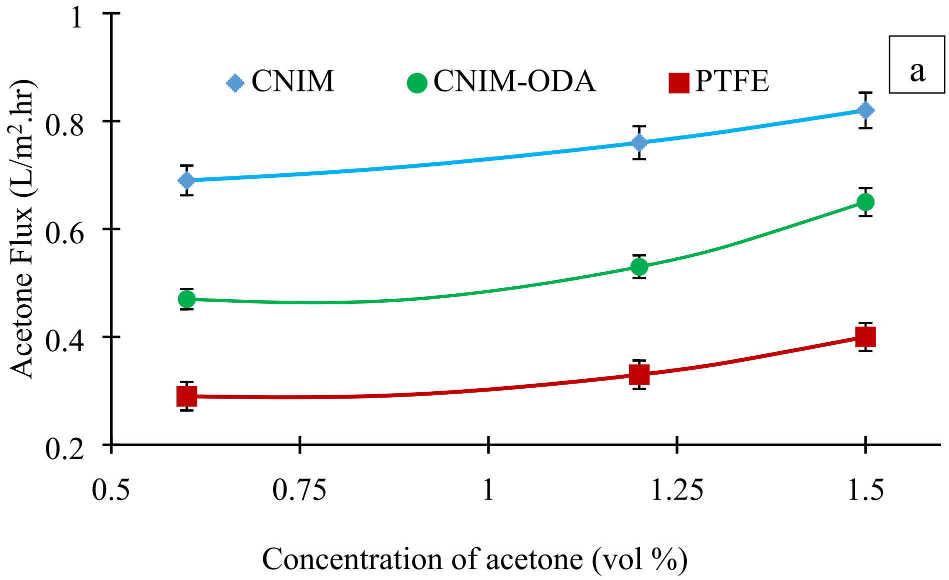
a
CNIM
CNIM-ODA
PTFE
Acetone Flux (L/m2.hr)
1
0.8
0.6
0.4
0.2
0.5
0.75
1
1.25
1.5
Concentration of acetone (vol %)

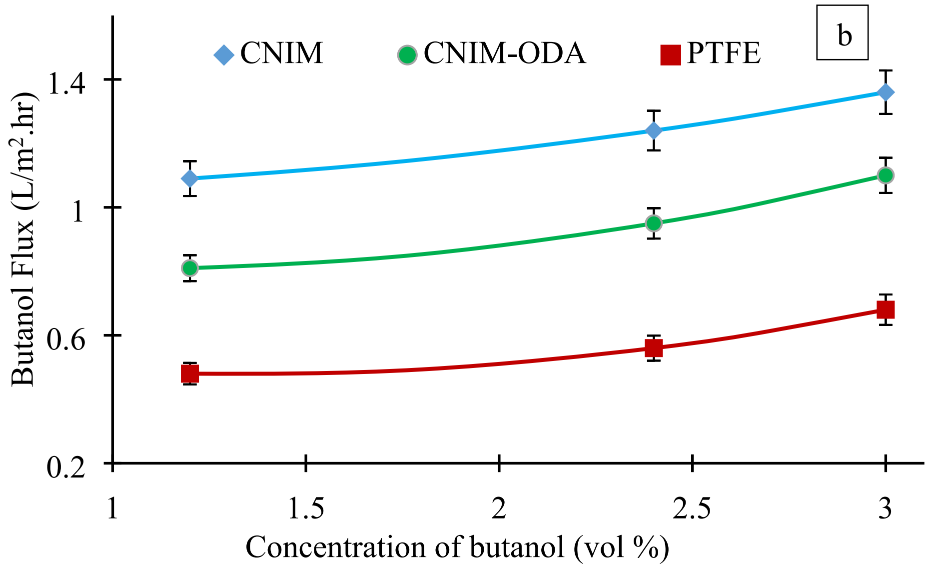
CNIM
CNIM-ODA
PTFE
b
Butanol Flux (L/m².hr)
1.4
1
0.6
0.2
1
1.5
2
2.5
3
Concentration of butanol (vol %)

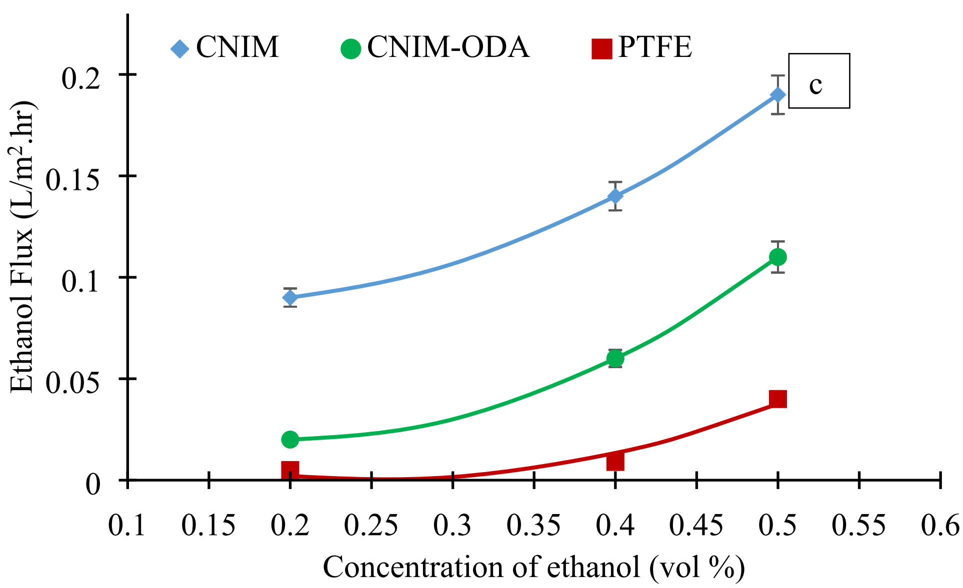
CNIM
CNIM-ODA
PTFE
c
Ethanol Flux (L/m².hr)
0.2
0.15
0.1
0.05
0
0.1
0.15
0.2
0.25
0.3
0.35
0.4
0.45
0.5
0.55
0.6
Concentration of ethanol (vol %)

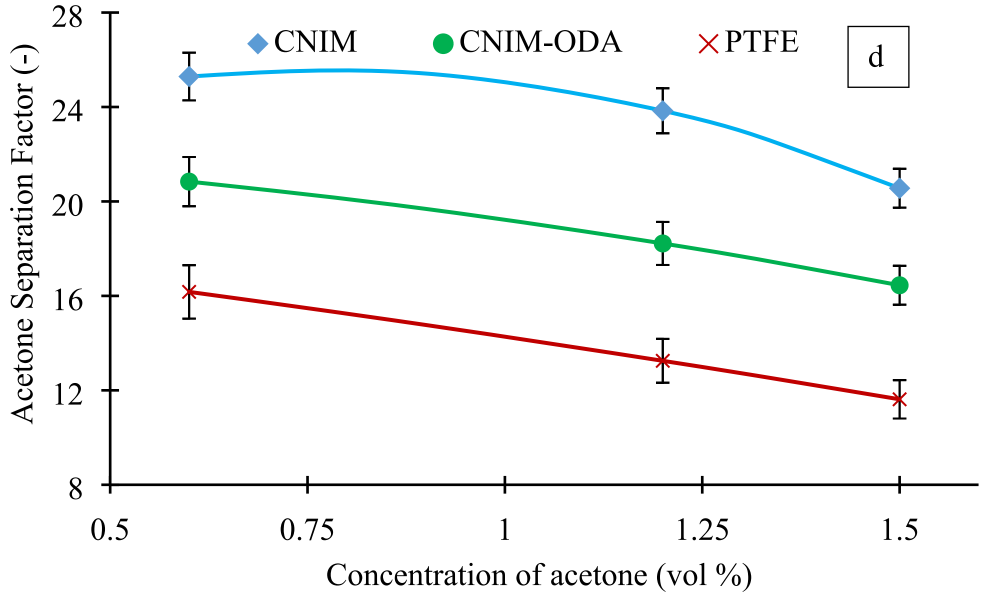

Acetone Separation Factor (-)
28
24
20
16
12
8
CNIM
CNIM-ODA
PTFE
d
0.5
0.75
1
1.25
1.5
Concentration of acetone (vol %)

273

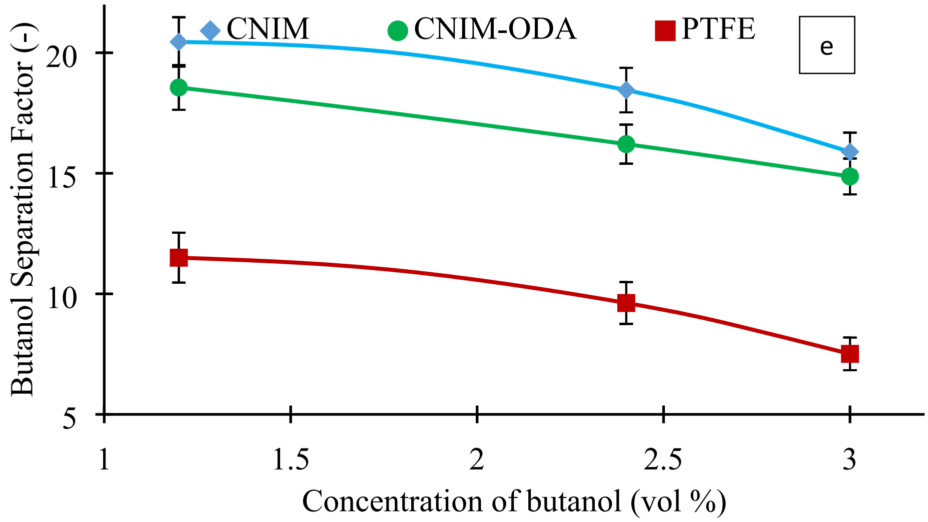

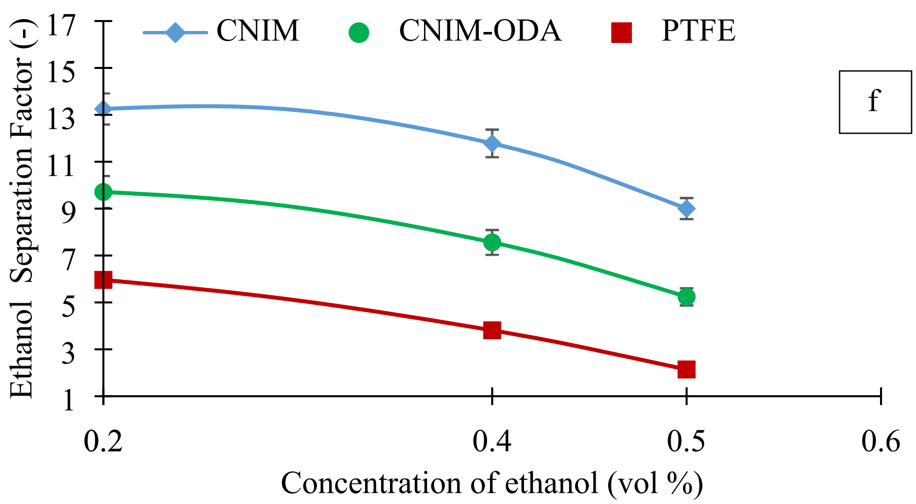

Figure 6. Effect of feed concentration on flux for (a) acetone, (b) butanol and (c) ethanol, and on separation factor for (d) acetone, (e) butanol and (f) ethanol

The acetone, butanol and ethanol flux and separation factor on the CNIM, CNIM-ODA and the PTFE membrane as a function of feed temperatures are demonstrated in Figures 7 a, b, c, d, e and f . A feed concentration of 1.5, 3 and 0.5 vol % of acetone, butanol and ethanol, respectively, was maintained and the feed flow rate was kept constant at 112 mL/min. The permeate fluxes for all membranes showed a direct relationship with feed temperature. At 60 ^{0}C, the CNIM flux reached up to 1.15 L/m^2.h, 1.54 L/m^2.h and 0.58 L/m^2.h for acetone, butanol and ethanol, respectively, which were considerably (around ten times) higher than previously reported data for pervaporation[43-44]. In general, higher fluxes at all temperatures for CNIM were observed followed by CNIM-ODA, although the enhancement was distinct at reduced temperature. At 40^{o}C the improvement in acetone, butanol and ethanol flux reached to 105, 100 and 375%, respectively, in comparison with pristine PTFE membrane. Hence, it is possible to perform the experiments at a relatively lower temperature thereby making it a less energy intensive process. It is well known that the vapor pressure increases exponentially with temperature and the sharp increase in vapor pressure from 40 to 60°C was reflected in the corresponding increase in ABE flux. From Figures 7 d, e and f, it can be observed that at all the operating temperatures; CNIM's separation performance was significantly better compared to the commercial PTFE membrane. The separation factor enhancement of CNIM compared to PTFE membrane reached to 103, 129 and 324% at 50^{o}C for ABE. As a result of negative effects of viscosity, a decline in ABE separation factor was observed with increase in operating temperatures for all membranes [45]. The water flux is presented in Figure 7g which showed an increase with feed temperature due to higher vapor pressure at elevated temperatures.

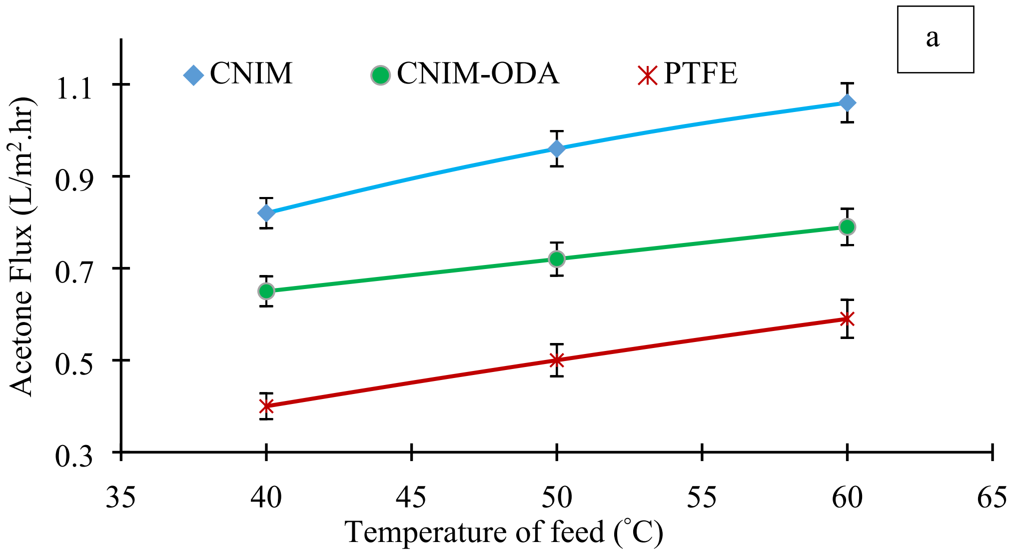
a
CNIM
CNIM-ODA
PTFE
Acetone Flux (L/m^2.hr)
1.1
0.9
0.7
0.5
0.3
35
40
45
50
55
60
65
Temperature of feed (˚C)

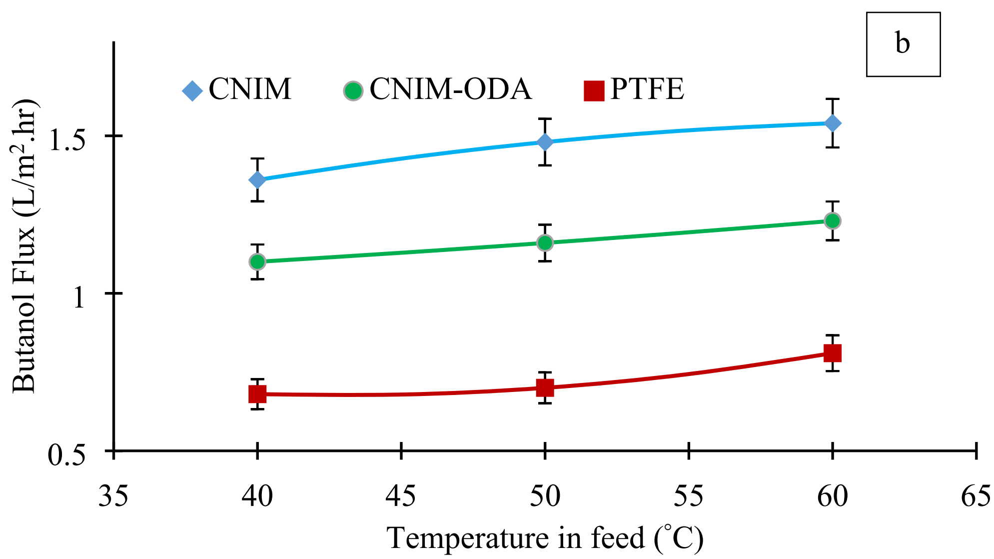
b
CNIM
CNIM-ODA
PTFE
Butanol Flux (L/m^2.hr)
1.5
1
0.5
35
40
45
50
55
60
65
Temperature in feed (˚C)

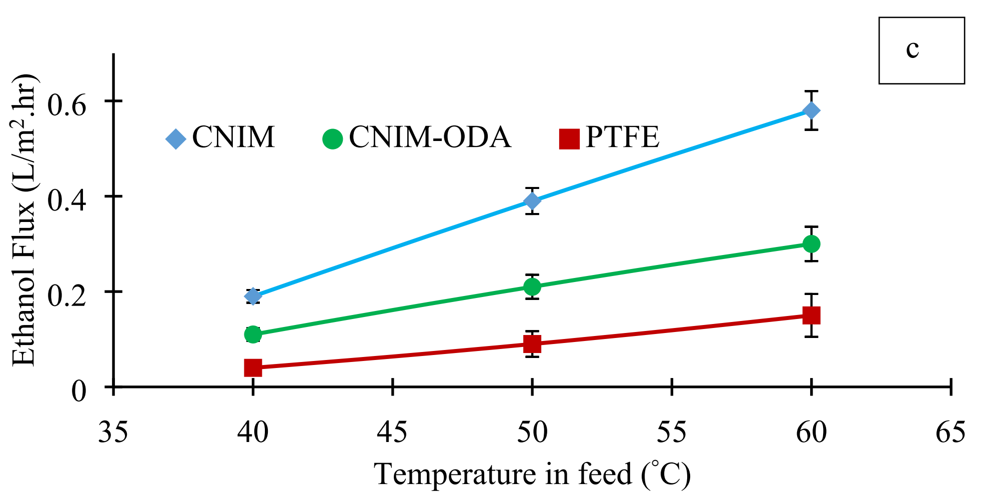
c
CNIM
CNIM-ODA
PTFE
Ethanol Flux (L/m^2.hr)
0.6
0.4
0.2
0
35
40
45
50
55
60
65
Temperature in feed (˚C)

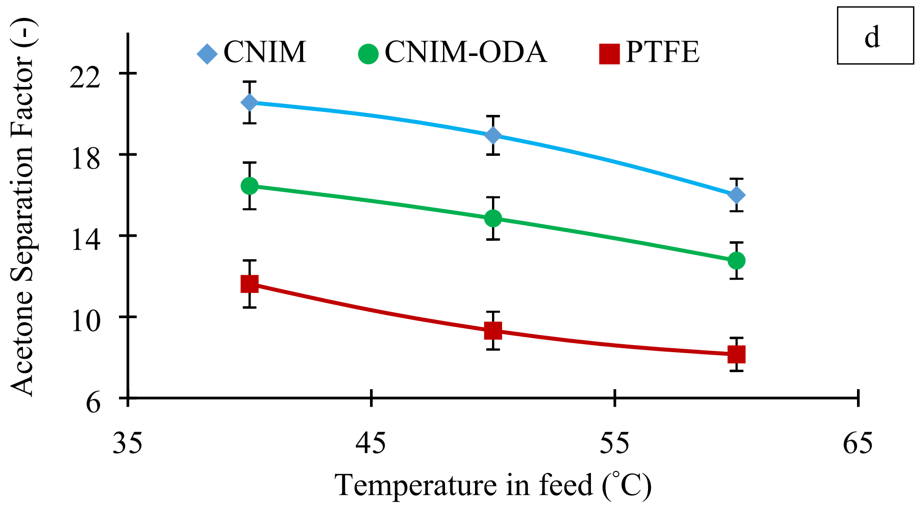
d
CNIM
CNIM-ODA
PTFE
Acetone Separation Factor (-)
6
10
14
18
22
35
45
55
65
Temperature in feed (˚C)

303

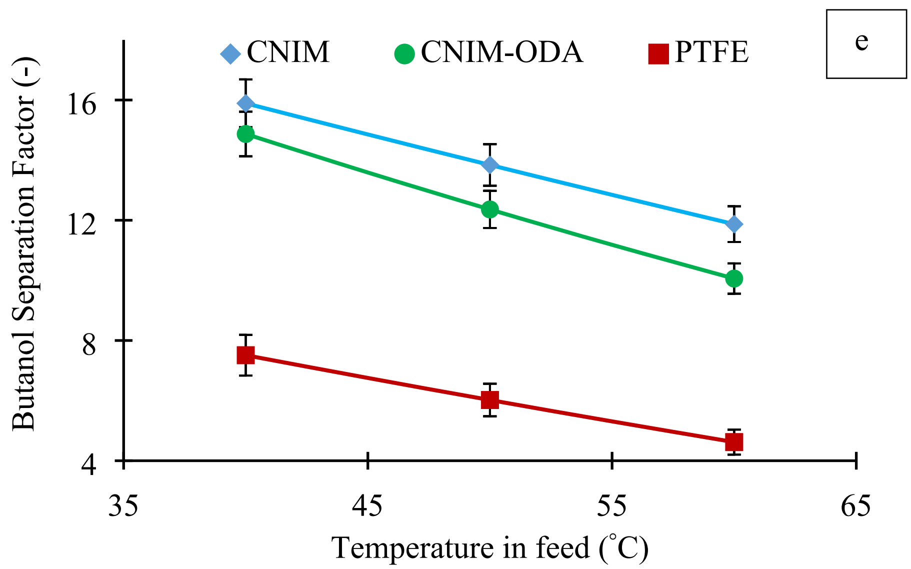
e
CNIM
CNIM-ODA
PTFE
Butanol Separation Factor (-)
4
8
12
16
35
45
55
65
Temperature in feed (˚C)

304

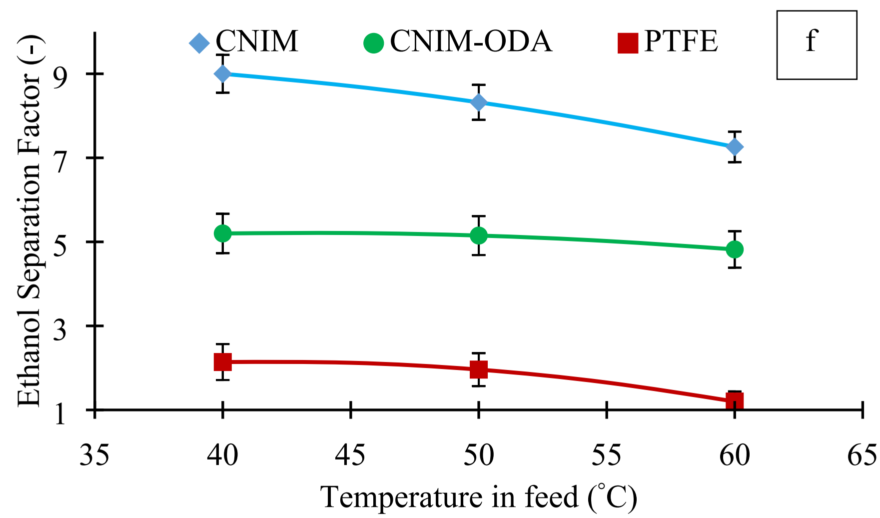

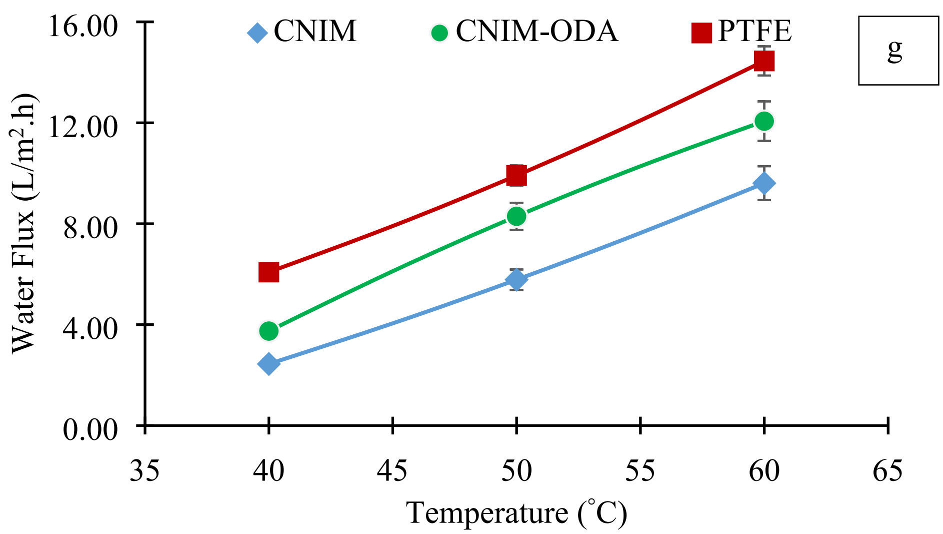

Figure 7. Effect of feed temperature on flux for (a) acetone, (b) butanol, (c) ethanol, and on separation factor for (d) acetone, (e) butanol, (f) ethanol, (g) effect of feed temperature on water flux

Apparent activation energy (E_{app}) for organic solvent transport through porous membranes in SGMD mode was calculated from Eq. (4). The concentration of the acetone, butanol and ethanol mixture was kept constant (1.5, 3, 0.5 vol %, respectively). The E_{app} values for PTFE, CNIM & CNIM-ODA are shown in Table 2.

Table 2. Apparent activation energy (E_{app}) values for acetone (1.5 vol%), butanol (3 vol%), ethanol (0.5 vol%) and water (95 vol %) in feed.

Membranes	Apparent activation energy (kJ/mol)			
	Acetone	Butanol	Ethanol	Water
PTFE	16.9	17.5	57.4	37.6
CNIM	11.2	5.4	48.5	59.5
CNIM-ODA	8.5	4.8	43.6	50.9

It is clear from the table that the presence of CNTs significantly reduced the apparent activation energy for all ABE components. Among three solvents, butanol exhibited the lowest E_{app} value followed by acetone and ethanol with all membranes. However, the activation energy of water was much higher which may be due to the exponential increment of water vapor pressure at elevated temperatures in case of modified membranes. This also results in reduction of separation factor with increase in feed temperature.

It was important to investigate if separation of each ABE component was affected by the presence of the other solvents. Therefore, binary mixture of each compound with water was also studied using PTFE and CNIM. The data related to the binary mixtures is presented in Figures 8a, b and c, where the flux of each component and separation factor are presented as a function of solvent concentration. The feed flow rate and the operating temperature was maintained at 112 mL/min and 40 °C, respectively. It is clear from the figure that with increase in feed concentration, the flux increased for each compound in both membranes. Butanol which had limited miscibility with water showed higher flux than ethanol that was significantly more miscible. As expected, higher flux was obtained for all solvents when CNIM was used. It was observed that the individual solvent flux in the binary mixtures were higher compared to the

ABE mixture under similar condition. For example, the acetone flux was obtained to be 1.36 $L/m^2.hr$ for CNIM at 40 ^0C and 1.5 vol % of acetone in water, which was 65.8% higher than the corresponding ABE mixture. Similar trend was also observed for butanol and ethanol mixture. The flux decline in the case of a mixture may be attributed to the mutual interaction and competition between the different compounds that reduced partitioning as well as permeability[46].

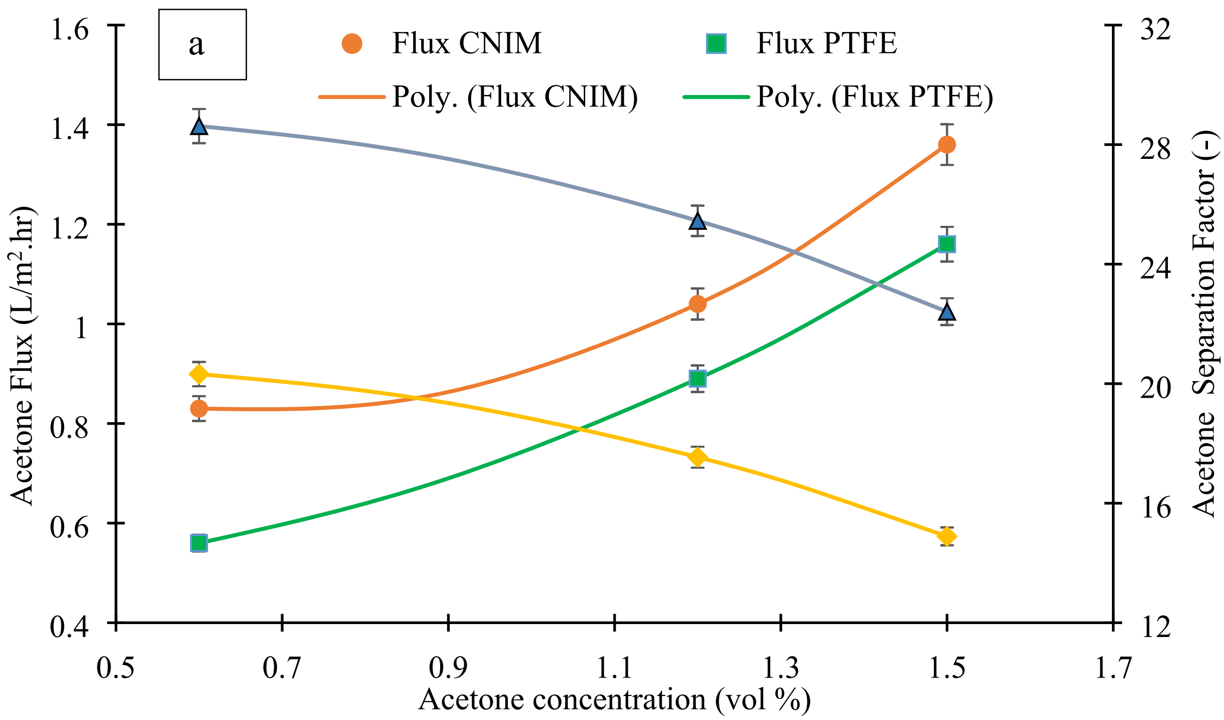

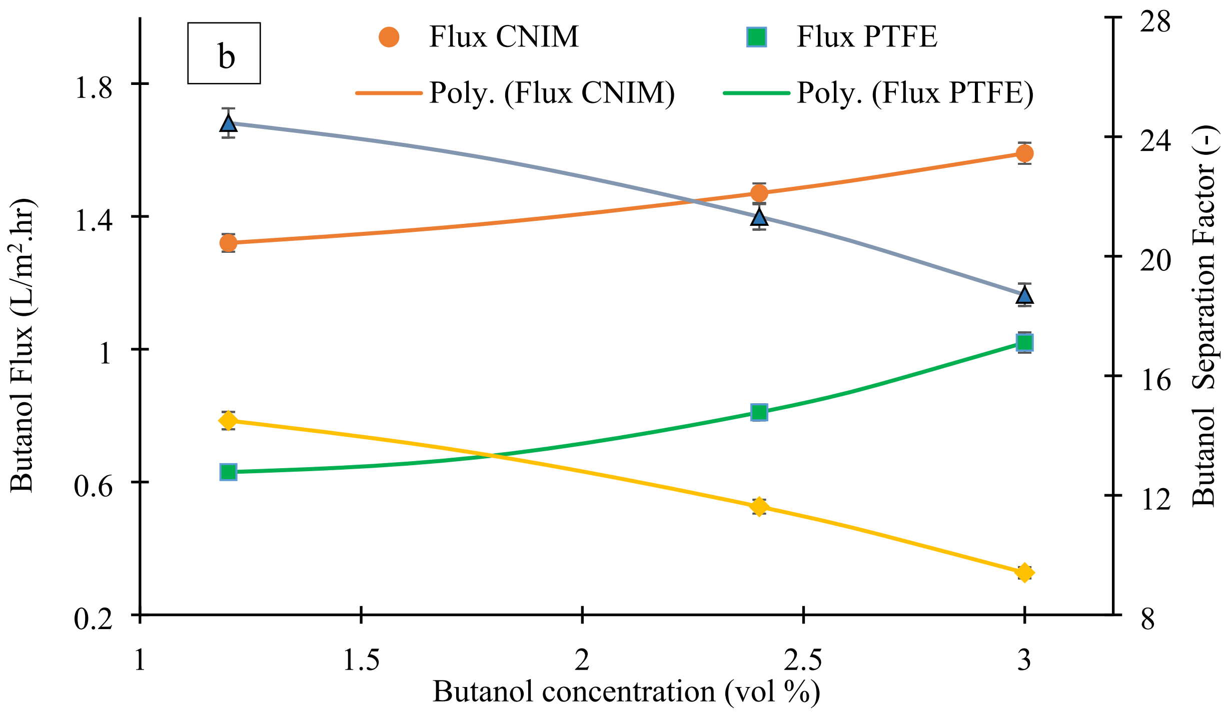

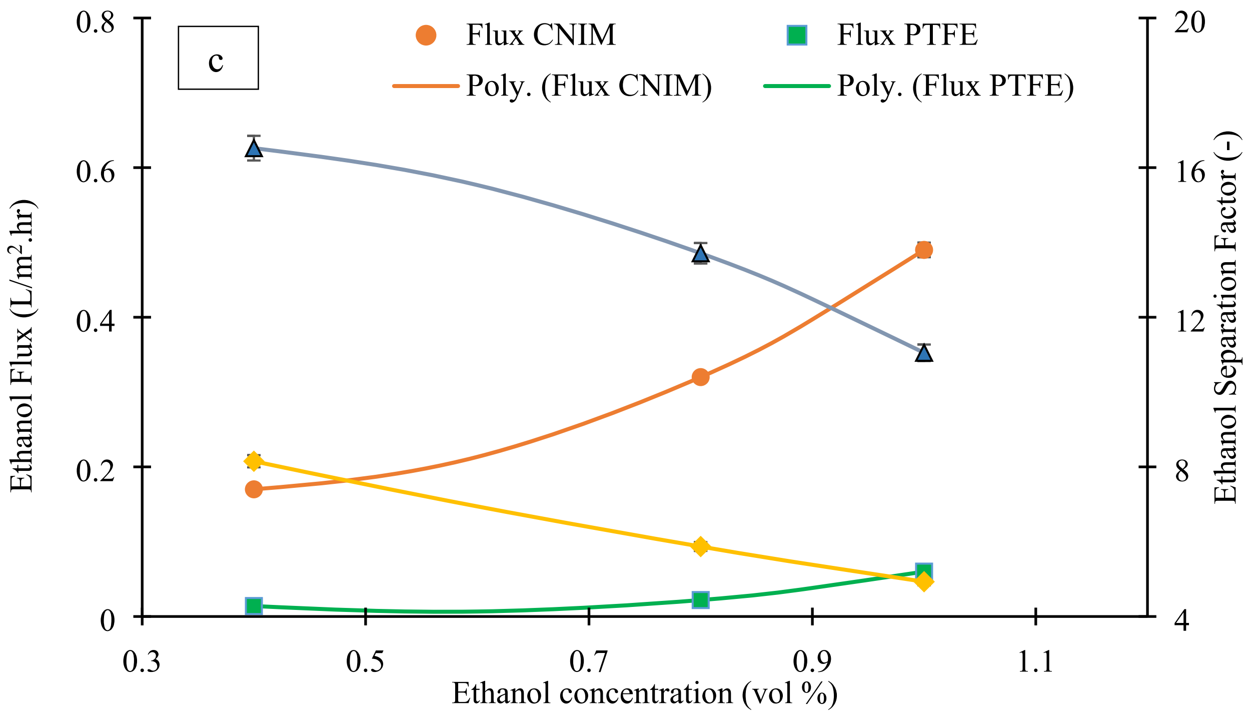

Figure 8. Effect of feed concentration on flux and separation factor for (a) acetone, (b) butanol, (c) ethanol

4. Mass transfer coefficient

The mass transfer coefficient (k) can be calculated from the following equation:

$$J_{wi} = k(P_{fi} - P_{pi}) \qquad (5)$$

$$k = \frac{J_{wi}}{P_{fi}} \qquad (6)$$

Where, J_{wi} is the flux of species 'i' and the feed side and permeate side partial vapor pressure is denoted as P_{fi} and P_{pi}, respectively. The vapor pressure of the different feed components at a particular temperature was attained from other sources [47] and the P_{pi}, was considered to be almost zero as the sweep air was dried completely prior to entering the permeate side of the membrane.

The 'k_i' values of different components in ABE mixture at varied operating temperatures and a constant feed flowrate of 112 mL/min are presented in Table 3. The mass transfer coefficients decreased or remained almost constant with increase in operating temperature for CNIM, CNIM-ODA and PTFE membranes. At all feed temperatures, the CNIM exhibited higher 'k_i' than the pristine PTFE membrane and CNIM-ODA. The enhancement of mass transfer coefficient over PTFE reached as high as 105% for CNIM and 62.5% for CNIM-ODA for acetone, 100 % and 61.8% for butanol and 375% & 175% for ethanol at 40 ^{0}C. For Butanol, the mass transfer coefficient follows an inverse relationship with temperature for all membranes. Also it is known that at higher temperatures the temperature polarization increases significantly, resulting in a lower membrane mass transfer coefficient [48].

Table 3. Mass transfer coefficient of ABE at different temperature and 1.5, 3 & 0.5 vol % ABE feed at 112 mL/min.

Temp (°C)	Mass transfer coefficient (x 10^{-3} L/m^2.h.mm-Hg)								
	PTFE			CNIM			CNIM-ODA		
	Acetone	Butanol	Ethanol	Acetone	Butanol	Ethanol	Acetone	Butanol	Ethanol
40	0.95	35.9	0.30	1.94	71.9	1.42	1.54	58.1	0.82
50	0.97	20.2	0.41	1.57	42.7	1.77	1.18	33.5	0.95
60	0.68	13.4	0.43	1.23	25.4	1.65	0.73	20.3	0.86

5. Membrane stability and proposed mechanism

To explore the stability of the membranes in presence of these strong organic solvents, SGMD experiments were performed for 8 h a day for 60 days with 1.5, 3 and 0.5 vol % of ABE concentration, respectively. The temperature was maintained at 60°C. The ABE flux was measured periodically. No substantial alteration in flux and membrane wetting were detected even during extended use for all membranes. It can be assumed that there was no significant CNTs loss from the membrane surface as it was not detected in the recycled feed solutions. Comparable stability checks in the past had been implemented where CNIM was used in high temperature aqueous solutions for extended periods and then examined for CNT loss [24].

Figure 9b demonstrates the enhanced ABE transport mechanism with CNIM. Earlier research published with CNTs have validated that CNTs are exceptional sorbents that increase solute partition coefficient generating higher permeation rate through the membranes [49-52]. The CNTs are also known to facilitate fast mass transport in both separation processes including chromatography, sorbents and membranes [53-55]. The higher vapor pressure of acetone, butanol and ethanol compared to water helped in selective sorption and penetration of ABE mixture through the porous membrane at low temperature. Apart from vapor-liquid equilibrium, the separation performance of CNTs incorporated membranes are due to improved sorption and activated diffusion of organic species on the frictionless CNTs. In addition it is worth noting that during conventional heating, the entire volume of the feed stream is uniformly heated whereas microwave heating results in localized superheating of the feed mixtures[56]. The dielectric loss of organic molecules is believed to increase with temperature whereas for water it decreases with temperature. This results in microwave dissipation being more significant in areas that are more heated and can lead to local turbulence and spatial temperature gradients[57]. A schematic of breakdown of the H-bonded solvent-water clusters is shown in Figure 9a. The localized super heating and breakdown of hydrogen bonded ABE–water clusters are likely to improve the tendency of solvent molecules to escape from the system, thus improving flux and separation efficiency. The significant enhancement in ABE flux and separation factors in CNIM and CNIM-ODA are attributed to these multiple factors.

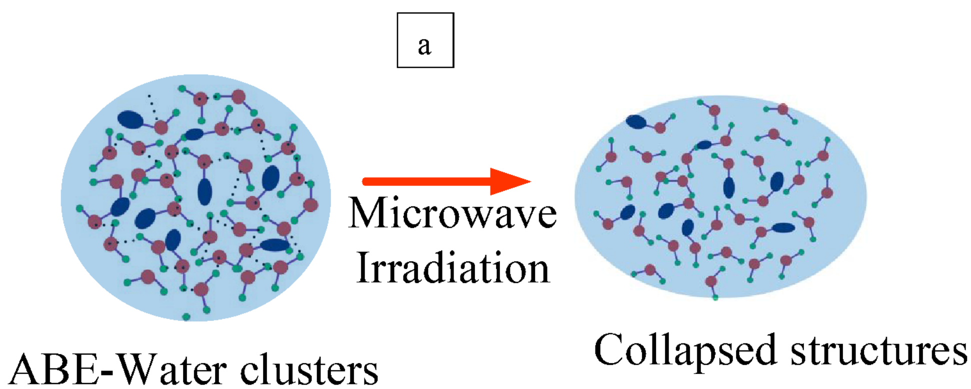

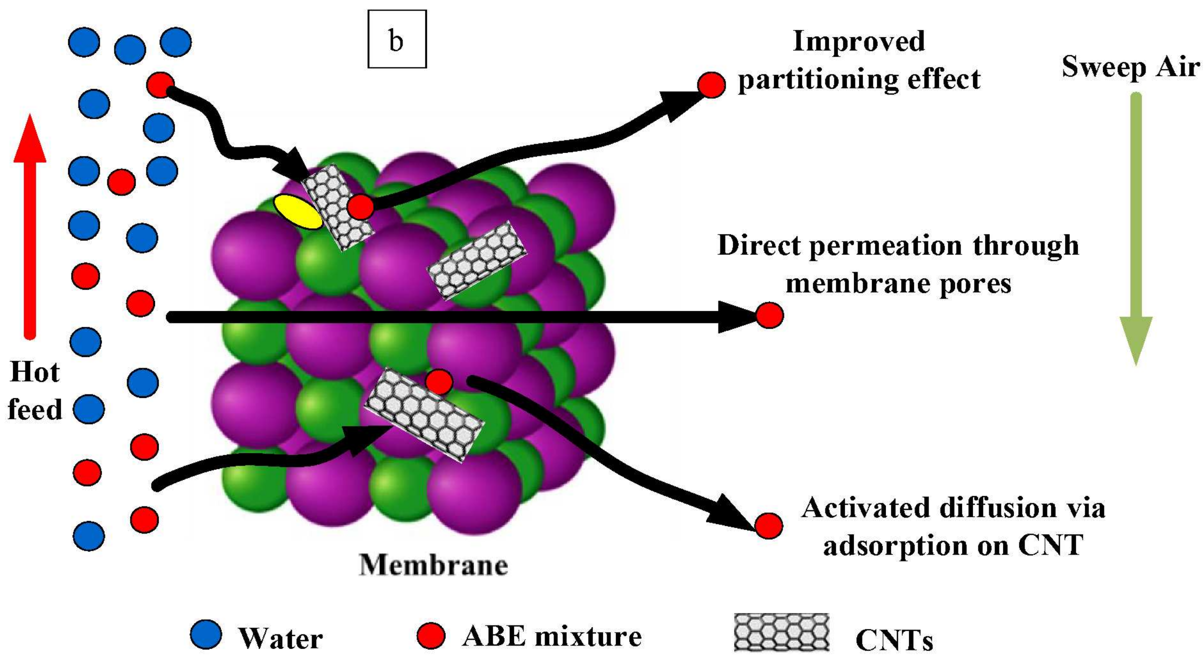

Figure 9 (a) H-Bonded ABE-Water clusters; (b) Proposed Mechanism Schematic

6. Concluding remarks

ABE separation is an important process in the economic development of biofuels with a goal of building a sustainable world economy. Several downstream processing techniques have been employed to recover ABE from its fermentation broth, however all these techniques suffer from various limitations. MIMD was investigated using CNT modified membranes, which showed significantly superior performance. Convectional thermal distillation is an expensive and energy intensive process and the MIMD based on CNIM is clearly a viable alternative. The separation of binary acetone-water, butanol-water and ethanol-water by the membranes were carried out initially to evaluate the membrane performance, which was found to follow the order of butanol>acetone> ethanol. The modified membranes were shown to be preferentially permeable to the ABE components. Improved partitioning and activated diffusion via CNT surface were factors that played important role in performance enhancement of the CNIM and CNIM-ODA. While modeling studies have shown some interesting results, this study for the first time demonstrates the viability of this technology in ABE recovery. As compared to the plain PTFE membrane, significant enhancement in ABE flux and separation factor were obtained with CNIM and CNIM-ODA membranes. The ABE flux obtained here is about ten times higher than that reported before for pervaporation, which is the only other reported membrane based technology for ABE recovery. Fermentation product recovery from the fermentation broth can be an important application for the modified CNT membranes.

Acknowledgement

The research was partially supported from a grant from NSF (CBET-1603314). Material Characterization Laboratory at Otto York Centre and financial support from the Ada Fritts Chair at NJIT are also acknowledged.

References:

1. Qureshi, N.; Ezeji, T. C., Butanol,'a superior biofuel'production from agricultural residues (renewable biomass): recent progress in technology. *Biofuels, Bioproducts and Biorefining: Innovation for a sustainable economy* **2008,** *2* (4), 319-330.
2. Ramanathan, K.; Koch, C. K.; Oh, S. H., Kinetic modeling of hydrocarbon adsorbers for gasoline and ethanol fuels. *Chemical engineering journal* **2012,** *207*, 175-194.
3. Rabelo, S.; Carrere, H.; Maciel Filho, R.; Costa, A., Production of bioethanol, methane and heat from sugarcane bagasse in a biorefinery concept. *Bioresource technology* **2011,** *102* (17), 7887-7895.
4. Gwaltney-Brant, S. M., Miscellaneous indoor toxicants. In *Small Animal Toxicology*, Elsevier: 2013; pp 291-308.
5. Ray, S.; Ray, S., Dehydration of acetic acid, alcohols, and acetone by pervaporation using acrylonitrile-maleic anhydride copolymer membrane. *Separation science and technology* **2005,** *40* (8), 1583-1596.
6. Peralta-Yahya, P. P.; Keasling, J. D., Advanced biofuel production in microbes. *Biotechnology journal* **2010,** *5* (2), 147-162.
7. Jain, M. K.; Beacom, D.; Datta, R., Mutant strain of C. acetobutylicum and process for making butanol. Google Patents: 1993.
8. Bankar, S. B.; Survase, S. A.; Ojamo, H.; Granström, T., Biobutanol: the outlook of an academic and industrialist. *Rsc Advances* **2013,** *3* (47), 24734-24757.
9. Gapes, J., The economics of acetone-butanol fermentation: theoretical and market considerations. *Journal of Molecular Microbiology and Biotechnology* **2000,** *2* (1), 27-32.
10. Ennis, B.; Qureshi, N.; Maddox, I., In-line toxic product removal during solvent production by continuous fermentation using immobilized Clostridium acetobutylicum. *Enzyme and Microbial Technology* **1987,** *9* (11), 672-675.
11. Ezeji, T.; Qureshi, N.; Blaschek, H., Acetone butanol ethanol (ABE) production from concentrated substrate: reduction in substrate inhibition by fed-batch technique and product inhibition by gas stripping. *Applied microbiology and biotechnology* **2004,** *63* (6), 653-658.
12. Qureshi, N.; Maddox, I. S., Continuous production of acetone-butanol-ethanol using immobilized cells of Clostridium acetobutylicum and integration with product removal by liquid-liquid extraction. *Journal of fermentation and bioengineering* **1995,** *80* (2), 185-189.
13. Grobben, N. G.; Eggink, G.; Cuperus, F. P.; Huizing, H. J., Production of acetone, butanol and ethanol (ABE) from potato wastes: fermentation with integrated membrane extraction. *Applied Microbiology and Biotechnology* **1993,** *39* (4-5), 494-498.
14. Qureshi, N.; Blaschek, H. P., Production of acetone butanol ethanol (ABE) by a hyper-producing mutant strain of Clostridium beijerinckii BA101 and recovery by pervaporation. *Biotechnology progress* **1999,** *15* (4), 594-602.
15. Kujawska, A.; Kujawski, J. K.; Bryjak, M.; Cichosz, M.; Kujawski, W., Removal of volatile organic compounds from aqueous solutions applying thermally driven membrane processes. 2. Air gap membrane distillation. *Journal of Membrane Science* **2016,** *499*, 245-256.
16. Garcia III, A.; Iannotti, E. L.; Fischer, J. L., Butanol fermentation liquor production and separation by reverse osmosis. *Biotechnology and bioengineering* **1986,** *28* (6), 785-791.
17. Roy, S.; Ragunath, S., Emerging membrane technologies for water and energy sustainability: Future prospects, constraints and challenges. *Energies* **2018,** *11* (11), 2997.
18. Banat, F.; Al-Shannag, M., Recovery of dilute acetone–butanol–ethanol (ABE) solvents from aqueous solutions via membrane distillation. *Bioprocess Engineering* **2000,** *23* (6), 643-649.

19. Banat, F.; Al-Rub, F.; Shannag, M., Simultaneous removal of acetone and ethanol from aqueous solutions by membrane distillation: prediction using the Fick's and the exact and approximate Stefan-Maxwell relations. *Heat and mass transfer* **1999,** *35* (5), 423-431.

20. Kujawska, A.; Kujawski, J.; Bryjak, M.; Kujawski, W., Removal of volatile organic compounds from aqueous solutions applying thermally driven membrane processes. 1. Thermopervaporation. *Chemical Engineering and Processing: Process Intensification* **2015,** *94*, 62-71.

21. Roy, S.; Ntim, S. A.; Mitra, S.; Sirkar, K. K., Facile fabrication of superior nanofiltration membranes from interfacially polymerized CNT-polymer composites. *Journal of membrane science* **2011,** *375* (1-2), 81-87.

22. Ong, Y. T.; Ahmad, A. L.; Zein, S. H. S.; Sudesh, K.; Tan, S. H., Poly (3-hydroxybutyrate)-functionalised multi-walled carbon nanotubes/chitosan green nanocomposite membranes and their application in pervaporation. *Separation and Purification Technology* **2011,** *76* (3), 419-427.

23. Gupta, O.; Roy, S.; Mitra, S., Enhanced membrane distillation of organic solvents from their aqueous mixtures using a carbon nanotube immobilized membrane. *Journal of Membrane Science* **2018,** *568*, 134-140.

24. Roy, S.; Bhadra, M.; Mitra, S., Enhanced desalination via functionalized carbon nanotube immobilized membrane in direct contact membrane distillation. *Separation and Purification Technology* **2014,** *136*, 58-65.

25. Kumar, M.; Ulbricht, M., Novel antifouling positively charged hybrid ultrafiltration membranes for protein separation based on blends of carboxylated carbon nanotubes and aminated poly (arylene ether sulfone). *Journal of membrane science* **2013,** *448*, 62-73.

26. Shi, Z.; Zhang, W.; Zhang, F.; Liu, X.; Wang, D.; Jin, J.; Jiang, L., Ultrafast separation of emulsified oil/water mixtures by ultrathin free-standing single-walled carbon nanotube network films. *Advanced materials* **2013,** *25* (17), 2422-2427.

27. Gu, J.; Xiao, P.; Chen, J.; Zhang, J.; Huang, Y.; Chen, T., Janus polymer/carbon nanotube hybrid membranes for oil/water separation. *ACS applied materials & interfaces* **2014,** *6* (18), 16204-16209.

28. Roy, S.; Singha, N., Polymeric nanocomposite membranes for next generation pervaporation process: Strategies, challenges and future prospects. *Membranes* **2017,** *7* (3), 53.

29. Bhadra, M.; Roy, S.; Mitra, S., A bilayered structure comprised of functionalized carbon nanotubes for desalination by membrane distillation. *ACS applied materials & interfaces* **2016,** *8* (30), 19507-19513.

30. Bhadra, M.; Roy, S.; Mitra, S., Enhanced desalination using carboxylated carbon nanotube immobilized membranes. *Separation and Purification Technology* **2013,** *120*, 373-377.

31. Nthunya, L. N.; Gutierrez, L.; Derese, S.; Nxumalo, E. N.; Verliefde, A. R.; Mamba, B. B.; Mhlanga, S. D., A review of nanoparticle-enhanced membrane distillation membranes: membrane synthesis and applications in water treatment. *Journal of Chemical Technology & Biotechnology* **2019**.

32. Yang, D.; Cheng, C.; Bao, M.; Chen, L.; Bao, Y.; Xue, C., The pervaporative membrane with vertically aligned carbon nanotube nanochannel for enhancing butanol recovery. *Journal of membrane science* **2019,** *577*, 51-59.

33. Kryachko, E. S., Ab initio studies of the conformations of water hexamer: modelling the penta-coordinated hydrogen-bonded pattern in liquid water. *Chemical physics letters* **1999,** *314* (3-4), 353-363.

34. Wang, L.; Miao, X.; Pan, G., Microwave-induced interfacial nanobubbles. *Langmuir* **2016,** *32* (43), 11147-11154.

35. Humoud, M. S.; Intrchom, W.; Roy, S.; Mitra, S., Reduction of scaling in microwave induced membrane distillation on a carbon nanotube immobilized membrane. *Environmental Science: Water Research & Technology* **2019,** *5* (5), 1012-1021.

36. Gupta, O.; Roy, S.; Mitra, S., Microwave Induced Membrane Distillation for Enhanced Ethanol–Water Separation on a Carbon Nanotube Immobilized Membrane. *Industrial & Engineering Chemistry Research* **2019,** *58* (39), 18313-18319.

37. Abramovitch, R. A., Applications of microwave energy in organic chemistry. A review. *Organic preparations and procedures international* **1991,** *23* (6), 683-711.

38. Reuß, J.; Bathen, D.; Schmidt-Traub, H., Desorption by microwaves: mechanisms of multicomponent mixtures. *Chemical engineering & technology* **2002,** *25* (4), 381-384.

39. Roy, S.; Petrova, R. S.; Mitra, S., Effect of carbon nanotube (CNT) functionalization in epoxy-CNT composites. *Nanotechnology reviews* **2018,** *7* (6), 475-485.

40. Bhadra, M.; Roy, S.; Mitra, S., Flux enhancement in direct contact membrane distillation by implementing carbon nanotube immobilized PTFE membrane. *Separation and Purification Technology* **2016,** *161*, 136-143.

41. Olatunji, S. O.; Camacho, L. M., Heat and Mass Transfer in Modeling Membrane Distillation Configurations: A Review. *Frontiers in Energy Research* **2018,** *6*, 130.

42. Kujawa, J.; Cerneaux, S.; Koter, S.; Kujawski, W., Highly efficient hydrophobic titania ceramic membranes for water desalination. *ACS Applied Materials & Interfaces* **2014,** *6* (16), 14223-14230.

43. Liu, F.; Liu, L.; Feng, X., Separation of acetone–butanol–ethanol (ABE) from dilute aqueous solutions by pervaporation. *Separation and Purification Technology* **2005,** *42* (3), 273-282.

44. Van Wyk, S.; Van Der Ham, A.; Kersten, S., Pervaporative separation and intensification of downstream recovery of acetone-butanol-ethanol (ABE). *Chemical Engineering and Processing-Process Intensification* **2018,** *130*, 148-159.

45. Lee, C. H.; Hong, W. H., Effect of operating variables on the flux and selectivity in sweep gas membrane distillation for dilute aqueous isopropanol. *Journal of Membrane Science* **2001,** *188* (1), 79-86.

46. Zhou, H.; Su, Y.; Chen, X.; Wan, Y., Separation of acetone, butanol and ethanol (ABE) from dilute aqueous solutions by silicalite-1/PDMS hybrid pervaporation membranes. *Separation and Purification Technology* **2011,** *79* (3), 375-384.

47. Parks, G. S.; Barton, B., Vapor pressure data for isopropyl alcohol and tertiary butyl alcohol. *Journal of the American Chemical Society* **1928,** *50* (1), 24-26.

48. Phattaranawik, J.; Jiraratananon, R., Direct contact membrane distillation: effect of mass transfer on heat transfer. *Journal of Membrane Science* **2001,** *188* (1), 137-143.

49. Roy, S.; Hussain, C. M.; Mitra, S., Carbon nanotube-immobilized super-absorbent membrane for harvesting water from the atmosphere. *Environmental Science: Water Research & Technology* **2015,** *1* (6), 753-760.

50. Ragunath, S.; Mitra, S., Carbon nanotube immobilized composite hollow fiber membranes for extraction of volatile organics from air. *The Journal of Physical Chemistry C* **2015,** *119* (23), 13231-13237.

51. Agnihotri, S.; Rood, M. J.; Rostam-Abadi, M., Adsorption equilibrium of organic vapors on single-walled carbon nanotubes. *Carbon* **2005,** *43* (11), 2379-2388.

52. Hussain, C. M.; Saridara, C.; Mitra, S., Modifying the sorption properties of multi-walled carbon nanotubes via covalent functionalization. *Analyst* **2009,** *134* (9), 1928-1933.

53. Hussain, C. M.; Saridara, C.; Mitra, S., Self-assembly of carbon nanotubes via ethanol chemical vapor deposition for the synthesis of gas chromatography columns. *Analytical chemistry* **2010,** *82* (12), 5184-5188.

54. Intrchom, W.; Mitra, S., Analytical sample preparation, preconcentration and chromatographic separation on carbon nanotubes. *Current opinion in chemical engineering* **2017,** *16*, 102-114.

55. Verweij, H.; Schillo, M. C.; Li, J., Fast mass transport through carbon nanotube membranes. *small* **2007,** *3* (12), 1996-2004.

56. Hong, J.; Ta, N.; Yang, S.-g.; Liu, Y.-z.; Sun, C., Microwave-assisted direct photolysis of bromophenol blue using electrodeless discharge lamps. *Desalination* **2007,** *214* (1-3), 62-69.
57. Routray, W.; Orsat, V., Dielectric properties of concentration-dependent ethanol+ acids solutions at different temperatures. *Journal of Chemical & Engineering Data* **2013,** *58* (6), 1650-1661.

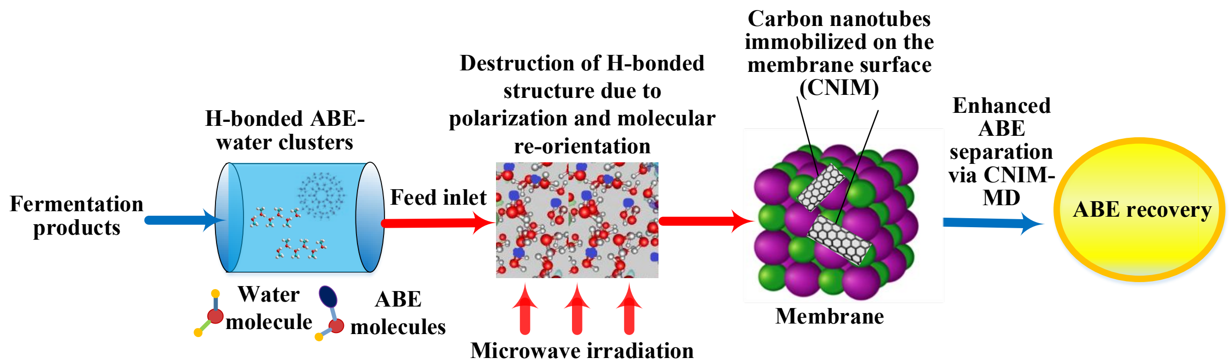

Text: Microwave Induced ABE separation via breakdown of H-Bonded ABE-water clusters and preferential adsorption of ABE on CNT surface